Method of assisting the fabrication process of holey fiber based on combination model of digital image processing and finite element method

Wenliang Lu(鹿文亮)[1,2] Shuqin Lou(娄淑琴)[1,2*] Liwen Wang(王立文)[1,2]
Weiguo Chen(陈卫国)[1,2]

[1] *Key Laboratory of All Optical Network & Advanced Telecommunication Network of EMC, Beijing Jiaotong University, Beijing* 100044, *China*
[2] *Institute of Lightwave Technology, Beijing Jiaotong University, Beijing* 100044, *China*
* *Corresponding author: shqlou@bjtu.edu.cn*

Received January 2, 2012; Accepted March 1, 2012

Abstract In the fabrication process of holey fiber, the final geometry of the actual fiber usually deviates from the ideal. We propose a novel method based on the combination of digital image processing technique and finite element method to model the optical properties of the actual fiber rapidly. A polarization-maintaining holey fiber reported by crystal fiber A/S has been modeled and its numerical results accord with the parameters given by the data. Experimental result demonstrates that the optical properties of the fiber can be analyzed rapidly so that the draw parameters can be adjusted in time.

Key words fiber optics; fabrication of holey fiber; digital image processing; finite element method (FEM)
OCIS codes 060.2280; 060.5295; 100.2000
doi: 10.3788/CJL201239.s105011

1 Introduction

Holey fibers, also known as photonic crystal fibers (PCFs), have novel optical properties such as endlessly single-mode behavior[1], highly birefringence[2], ultra-high nonlinear[3], large mode-area[4], ultra-flattened and anomalous dispersion[5] and so on. Those attractive characteristics make them a number of potential applications in fiber communication, fiber sensor, fiber devices, and so on[6].

PCFs are manufactured by heating a macroscopic structured preform (a few centimeters in diameter) and drawing it to the required dimension (typically 125 μm) with the drawing tower. The geometry of the final fiber can be modified significantly by controlling the parameters used in the drawing process, i.e., the temperature of the furnace, the feed speed at which the preform is fed into the furnace, and the draw speed. The control process is more complex, difficult, and time-consuming than that in the ordinary fiber fabrication. Slight parameter variation in the fabrication process would affect the geometry of the fiber. Up to now, there have been some studies on the fabrication process in order to optimize the drawing parameters[7]. However, even with the theoretical optimum drawing parameters in the fabrication process, there are also some deviations from the ideal PCF. In order to decrease the deviation of the optical properties between the actual fiber and the ideal one, it is crucial to monitor the properties of the actual fiber until its properties are steady before the coating process during fabrication so that the optimum drawing parameters in the fabrication process can be obtained. The conventional methods employed to measure the properties of the actual photonic crystal fiber often require long fiber samples, a long operating time and complex expensive equipments. These methods cannot meet the requirement that monitor the properties during the drawing process. Due to the length limit of the preform, it is important to optimum drawing parameters as soon as possible during the fabrication process. To our knowledge, there are few literatures about the method of modeling actual holey fibers and monitoring properties of the no-coated fibers at the beginning of the fabrication process.

In this paper, a novel method is developed to analyze actual holey fiber based on the combination model of digital image processing technique and finite element method (FEM). It can be used to analyze the actual fiber rapidly to optimize the drawing parameters from the analysis results and monitor the properties of the no-coated fiber whether to meet the requirement before the coating stage during the PCF fabrication process. Compared with conventional method which needs a long operating time, this method is more rapid and more significant to conduct the manufacture process.

2 Methodology

In order to model the properties of the actual PCF, a novel method was developed, which mainly includes

four steps as shown in Fig. 1.

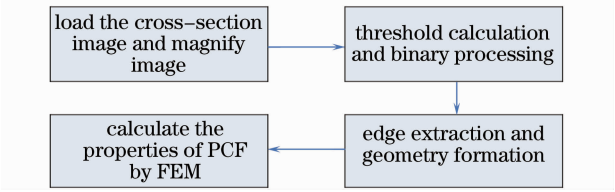

Fig. 1　Workflow of the methodology

The first step is to load the cross-section image and magnify the image. The ross-section image can be collected by digital microscope. In order to improve image recognition accuracy, image magnification is necessary. Figure 2 shows a cross-section image of a PCF and its enlarged image which is two times as the original one. Here, a typical method, i.e., the bi-cubic convolution interpolations[8], which is a cubic interpolation algorithm that give a quite well approximation of the theoretically optimum since interpolation function, has been applied and its schematic diagram is shown in Fig. 3.

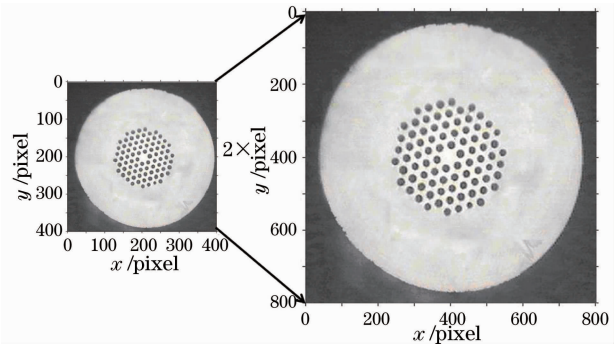

Fig. 2　Original cross-section image and its two times enlarged image

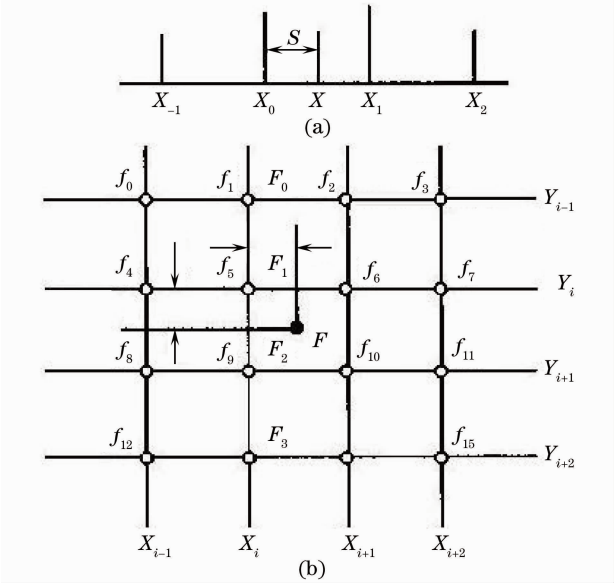

Fig. 3　Schematic diagram of the cubic convolution interpolation used for image enlarged

To assume that g is the corresponding interpolation function and f is a sampled function, then $g(x_k)=f(x_k)$ for any interpolation node x_k. For equally spaced data as shown in Fig. 3(a), the interpolation function $g(x)$ can be described by

$$g(x)=\sum_k c_k u\left(\frac{x-x_k}{h}\right), \tag{1}$$

where h represents the sampling increment such as $h=x_1-x_0$ and x_k is the interpolation nodes, u is the interpolation kernel, and g is the interpolation function. Depending upon the sampled data, parameters c_k are selected to satisfy the interpolation condition, $g(x_k)=f(x_k)$ for each x_k. Then the kernel of cubic convolution interpolation is built up with third-order polynomials and given by

$$u(s)=\begin{cases}\dfrac{3}{2}|s|^3-\dfrac{5}{2}|s|^2+1, & 0<|s|<1\\ -\dfrac{1}{2}|s|^3+\dfrac{5}{2}|s|^2-4|s|+2, & 1<|s|<2\\ 0, & 2<|s|\end{cases} \tag{2}$$

where $s=(x-x_0)/h$.

Introducing cubic convolution interpolation in digital image magnification is shown in Fig. 3(b). In order to get the pixel value of the interpolation point F, the pixel value of four temporary interpolation points (F_0, F_1, F_2, F_3) of every row should be calculated firstly with Eqs. (1) and (2). The pixel value of point F can be obtained by the four temporary points (F_0, F_1, F_2, F_3) of the column. This method is called the bi-cubic interpolation method, which is more accurate than others as reported in Ref. [8].

After the image magnification, the next step is threshold setup and binary processing which convert a grayscale into a binary image with only two colors, black (0) and white (1). The boundary of neighborhoods can be easily extracted from the binary image. The threshold setup is crucial to determine whether the extracted geometry of PCF can accurately represent the cross session of actual PCF. Based on the histogram in Fig. 4(a), the iterative threshold method is used to obtain the threshold. The method includes the following four steps.

Step 1: selecting an initial threshold T_0 which is better to be the average pixel gray of the image.

Step 2: individually calculating the mean pixel gray values of the parts separated by the iterative threshold T_k which is obtained from the last iteration,

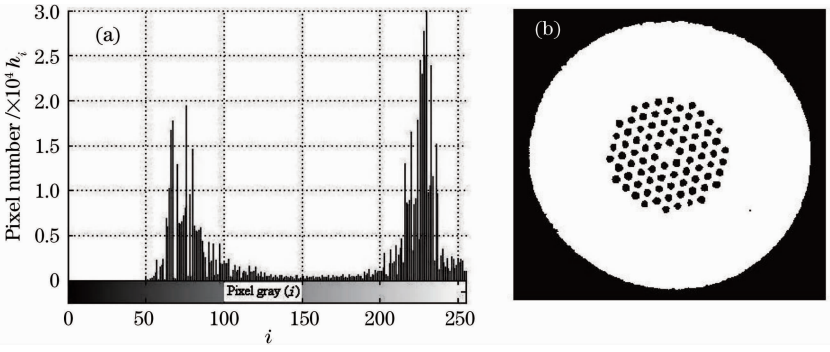

Fig. 4 (a) Histogram of the image shown in Fig. 2 used for threshold setup and binary processing; (b) binary image form the threshold setup and binary processing

$$\begin{cases} \mu_1 = \sum_{i=0}^{T_k} (h_i \times i) \Big/ \left(\sum_{i=0}^{T_k} h_i \right), \\ \mu_2 = \sum_{i=T_k}^{255} (h_i \times i) \Big/ \left(\sum_{i=T_k}^{255} h_i \right), \end{cases} \tag{3}$$

where i is the pixel gray range from 0 to 255, μ_1 and μ_2 are the mean pixel gray values of the corresponding parts, respectively.

Step 3: calculating the new threshold value T_{k+1} defined by

$$T_{k+1} = (\mu_1 + \mu_2)/2. \tag{4}$$

Step 4: repeating step 2 to step 3 until the threshold value T_k in successive iterations changes in an acceptable range. The final threshold setup is obtained.

Using the threshold calculated in step 4, a binary image shown in Fig. 4(b) can be set up from the enlarged cross-section image of PCF in Fig. 2.

With the binary image, the discrete edge, as shown in Fig. 5(a), can be extracted by the morphology which is a technique of image processing based on structuring elements. Then the least squares fitting method is used to deal with the discrete edges of each region. The geometry of the cross session of PCF is rebuilt in Fig. 5(b) in which the new coordinate system corresponding to the actual fiber is obtained by

$$\begin{cases} x_{\text{new}} = C(x_{\text{pixel}} - x_0), \\ y_{\text{new}} = C(y_{\text{pixel}} - y_0), \end{cases} \tag{5}$$

where the scaling coefficient C is denoted by the ratio of the outer diameter of the actual fiber to the pixels diameter which is defined as D. (x_0, y_0) are the center pixel of the geometry in the pixel coordinate system which can be obtained by the average of the discrete edge pixels in the outer diameter of fiber.

After the geometry of the cross session of the actual PCF is rebuilt, FEM is employed to model the properties of the actual PCF. Mesh generation is a key step in FEM. Here, we use the mesh generator in MatLab 7.0 to generate triangulation mesh which is denser in the center region and near the boundary in order to reduce the computing time and increase, accuracy, and then the properties of the actual PCF can be analyzed by FEM with second order interpolation function[9]. The effective refractive index and the distribution of modal field can be obtained directly, and thus other properties, such as the chromatic dispersion, mode-field area, nonlinear coefficient, and the beat length, can be deduced respectively.

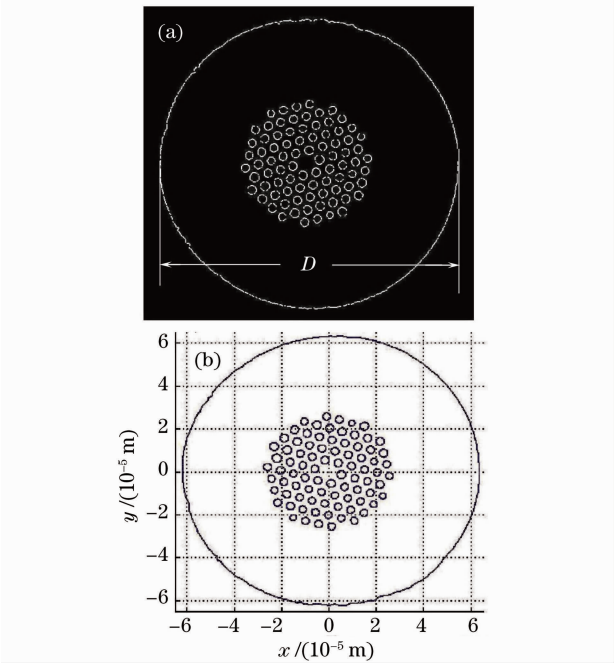

Fig. 5 (a) Binary edge of the air-holes and the fiber; (b) rebuilt geometry from the binary edge

3 Application of this method to model the outual PCF

With this method, the properties of a polarization maintaining PCF made by the crystal fiber A/S are mod-

eled. This PCF, as shown in Fig. 6(a), has hole-pitch of $\Lambda = 4.4$ μm and a hole diameter of $d_1 = 2.2$ μm for the small holes and $d_2 = 4.5$ μm for the large ones, the diameter of holey region is about 40 μm and the outside diameter is 125 μm[10]. The inner four rings holey region has been extracted and meshed as shown in Fig. 6 (b). Then, the properties are analyzed with FEM. Dispersion and beat length are shown in Fig. 7.

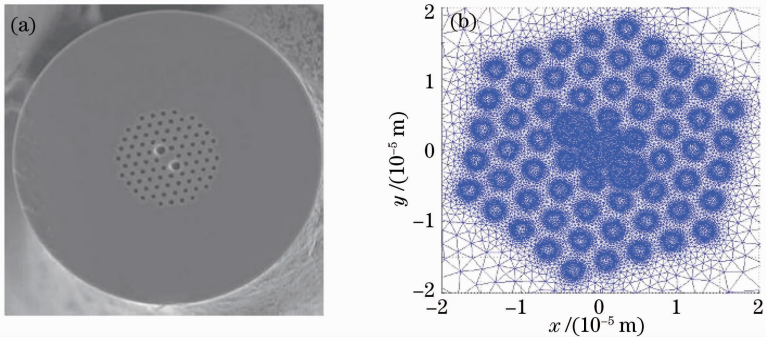

Fig. 6 (a) Cross-section and (b) mesh of the inner four rings air-holes of a polarization maintaining photonic crystal fiber

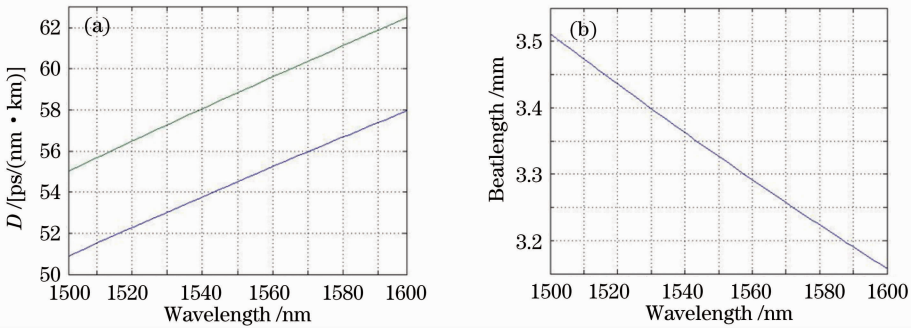

Fig. 7 (a) Dispersion and (b) beat length of the two fundamental polarizations mode

Numerical results by our method and the product data given by the crystal fiber A/S at the wavelength of 1550 nm[10] have been listed in Table 1. It is clear that the method we developed can model the actual PCF with high accuracy. When this tool runs on the computer with Intel P4 2.8 GHz and 2 G RAM, the whole process shown in Fig. 1 consumes about 3.4 min. The consuming time will decrease significantly using powerful computer. This means that the method can be used to monitor and optimize the drawing parameters rapidly before coating the fiber during the fabrication process.

Table 1 Comparisons of the numerical results with the product parameter

λ = 1550 nm	Dispersion of two polarizations		Beat length /mm
Given results	54	59	<4
Numerical results	54.5	58.8	3.33

Then we use this method to improve the fabrication process at the beginning stage of fabricating a new holey fiber. With theoretical and empirical drawing parameters, the cross section of the fabricated but no-coated single mode holey fiber is shown in Fig. 8(a). From the

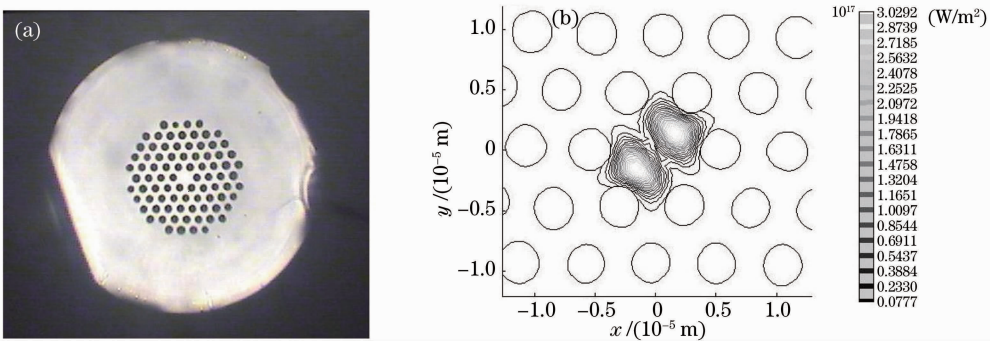

Fig. 8 (a) Cross-section image of a holey fiber which air holes are expanded; (b) power spectrum contour line map of this fiber's second order mode, the effective refractive index is $1.4343 - i8.6368e^{-13}$ and the confinement loss is $3e^{-5}$ dB/m

cross section, the properties of this actual fiber are analyzed with the above method. Numerical result demonstrates that the fiber can propagate not only the fundamental mode but also the second-order mode. The second-order mode is shown in Fig. 8(b). The properties deviate from the initial single mode design. Therefore, the drawing parameters in the fabrication process should be adjusted to obtain the single mode holey fiber. Guo *et al.* reported that the actual geometry of the holey fiber was affected by the furnace temperature and inert gas pressure[7]. Through decreasing these two parameters, the air holes diameter would be reduced. After adjusting the parameters, the actual fiber can be analyzed in time. As an example, Fig. 9(a) is a cross-section image of the fiber after parameters adjusting. The air holes' diameter is smaller than one shown in Fig. 8(a).

The second θ-order mode analyzed by the above method has been shown in Fig. 9(b). Its confinement loss is so large that its second-order mode fast attenuates and there is only fundamental mode existing in this fiber. Although the air holes are slightly larger than the designed one, the properties of the fiber meet our requirement. Therefore, the suitable drawing parameters for fabricating the single mode PCF are obtained and the consumed time can be reduced as well. The final fiber sample can be fabricated through coating the fiber under this draw condition. Experimental results demonstrate that this method can be used to optimize the drawing parameters before the fiber is coated in the fabrication process. This is a useful tool to improve the PCF fabrication technology and to provide required photonic crystal fibers for applications.

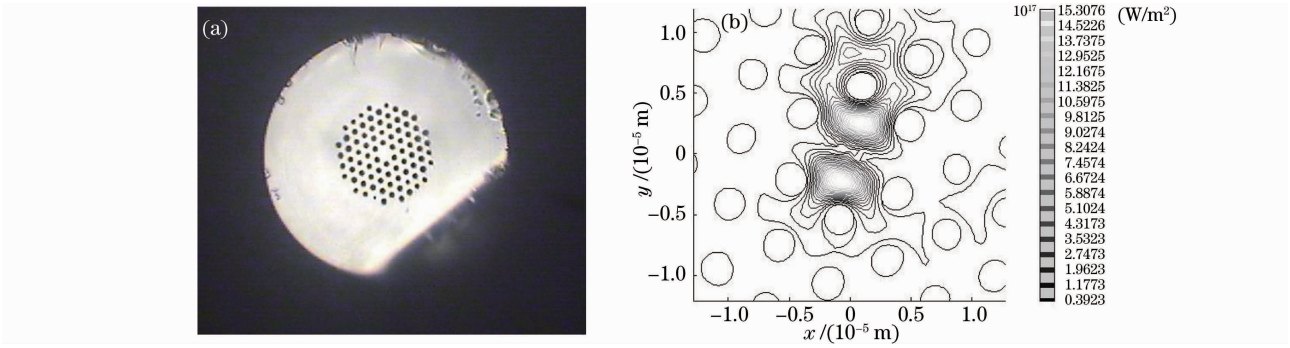

Fig. 9 (a) Cross-section image of a holey fiber after parameter adjustment; (b) power spectrum contour line map of this fiber's second order mode, as well as the effective refractive index is $1.4381 - i6.2440e^{-7}$ and the confinement loss is 21.99 dB/m

4 Conclusion

In this paper, a novel method of analyzing actual holey fibers based on a combination of digital image processing technique and FEM used for assisting the fabrication process is developed. Due to its accuracy and rapidity, this method can be used to optimize the drawing parameters and monitor the properties of the no-coated fiber whether to meet the requirements in order to reduce the consumed time during the PCF fabrication process. The length of the preform is limited, reducing the consumed time of optimizing the drawing parameters means that we have a higher probability to get the ideal PCF or get longer PCFs. This is a useful tool to improve the PCF fabrication technology and to provide required photonic crystal fibers for applications.

This work was supported by the State Key Development Program for Basic Research of China (No. 2010CB328206), the National Natural Science Foundation of China (No. 60977033) and the Foundamental Research Funds for the Central Universities (No. 2012YJS011).

References

1 T. A. Birks, J. C. Knight, P. St. J. Russell. Endlessly single-mode photonic crystal fiber[J]. *Opt. Lett.*, 1997, **22**: 961～963
2 A. Ortigosa-Blanche, J. C. Knight, W. J. Wadsworth *et al.*. Highly birefringent photonic crystal fibers[J]. *Opt. Lett.*, 2000, **25**: 1325～1327
3 W. J. Wadsworth, A. Ortigosa-Blanch, J. C. Knight *et al.*. Super-continuum generation in photonic crystal fibers and optical fiber tapers: a novel light source[J]. *J. Opt. Soc. Am. B*, 2002, **19**(9): 2148～2155
4 J. R. Folkenberg, M. D. Nielsen, N. A. Mortensen *et al.*. Polarization maintaining large mode area photonic crystal fiber[J]. *Opt. Express*, 2004, **12**: 956～960
5 J. C. Knight, J. Arriaga, T. A. Birks *et al.*. Anomalous dispersion in photonic crystal fiber[J]. *IEEE Photon. Technol. Lett.*, 2000, **12**(7): 807～809
6 T. A. Birks. Photonic crystal fibre devices[C]. *Proc. SPIE*, 2002, **4943**: 142～151
7 Tieying Guo. Control of the fabrication parameters during the fabrication of photonic crystal fibers[J]. *Chin. Phys. Soc.*, 2009, **58**(9): 412～419
8 H. S. Hou, H. C. Andrews. Cubic splines for image interpolation and digital filtering[J]. *IEEE Trans. Acoustics, Speech & Signal Proc.*, 1978, **26**(6): 508～517
9 P. Federica. Photonic Crystal Fiber-Properties and Application [M]. New York: Springer, 2007
10 Crystal fiber A/S. "Introduction of a polarisation maintaining PCF CPM|1550-01". http://www.crystal-fiber.com/datasheets/PM-1550-01.pdf